Interplay between topological insulators and superconductors

Jian Wang,[1,2,*] Cui-Zu Chang,[3,4] Handong Li,[5,6] Ke He,[3] Duming Zhang,[1] Meenakshi Singh,[1] Xu-Cun Ma,[3] Nitin Samarth,[1] Maohai Xie,[5] Qi-Kun Xue,[3,4] and M. H. W. Chan[1,†]

[1]*Center for Nanoscale Science and Department of Physics, Pennsylvania State University, University Park, Pennsylvania 16802-6300, USA*

[2]*International Center for Quantum Materials and State Key Laboratory for Mesoscopic Physics, School of Physics, Peking University, Beijing, 100871, China*

[3]*Institute of Physics, Chinese Academy of Sciences, Beijing 100190, China*

[4]*Department of Physics, Tsinghua University, Beijing 100084, China*

[5]*Physics Department, University of Hong Kong, Pokfulam Road, Hong Kong, China*

[6]*State Key Laboratory of Electronic Thin Films and Integrated Devices, University of Electronic Science and Technology of China, Chengdu, Sichuan, 610054, China*

(Received 14 December 2011; published 10 January 2012)

Topological insulators are insulating in the bulk but possess metallic surface states protected by time-reversal symmetry. Here, we report on a detailed electronic transport study in high-quality Bi_2Se_3 topological insulator thin films contacted by superconducting (In, Al, and W) electrodes. The resistance of the film shows an abrupt and significant upturn when the electrodes become superconducting. In turn, the Bi_2Se_3 film greatly weakens the superconductivity of the electrodes, significantly reducing both their transition temperatures and their critical fields. A possible interpretation of these results is that the superconducting electrodes are accessing the surface states and the experimental results are consequences of the interplay between the Cooper pairs of the electrodes and the spin-polarized current of the surface states in Bi_2Se_3.

DOI: 10.1103/PhysRevB.85.045415 PACS number(s): 73.25.+i, 03.65.Vf, 73.23.−b, 73.50.−h

I. INTRODUCTION

Bismuth-based materials have long been studied for their thermoelectric properties.[1–3] Bismuth selenide (Bi_2Se_3), bismuth antimonide ($Bi_{1-x}Sb_x$), bismuth telluride (Bi_2Te_3), and antimony telluride (Sb_2Te_3) have been predicted theoretically and confirmed experimentally by angle-resolved photoemission spectroscopy (ARPES) experiments to be three-dimensional (3D) topological insulators (TIs) because of strong spin–orbit interactions.[1–11] In transport measurements of 3D TIs,[12–19] quantum magnetoresistance (MR) oscillations have been observed and interpreted as evidence of a topologically protected surface state. Of these, Bi_2Se_3, with a simple surface state structure (a single Dirac cone) and relatively large band gap (0.3 eV) has become a reference material in 3D TIs. A key feature of the surface state is that the spin and momentum of the conduction electrons are locked,[4] which has been confirmed by ARPES measurements[20,21] but has not been directly demonstrated in transport experiments.

In this paper, we report on the transport behavior of crystalline Bi_2Se_3 films contacted by three kinds of superconducting electrodes to study the interplay between the superconductivity and the TI surface state. We use superconducting bulk indium (In) electrodes and mesoscopic aluminum (Al) and tungsten (W) electrodes to study the transport property of the Bi_2Se_3 films with thicknesses of 5 and 200 quintuple layers (QLs) on sapphire and silicon substrates, respectively. Every QL is 1 nm thick. A simple two-probe configuration is used to minimize the fabrication processing of the electrodes and hence to reduce the risk of altering the intrinsic property of the TI samples. The two-probe (pseudo–four-probe) geometry used here has two contact pads (wires) for each probe. The distances between superconducting electrodes are 1 mm (In) and 1 μm (Al and W). Irrespective of the material of the electrodes, the thickness of the Bi_2Se_3 film, the separation of electrodes, the substrates, and the contact resistance, the low-bias resistance shows a large and abrupt increase near the superconducting transition temperature (T_C) of the electrodes. Most interestingly, we observe that the Bi_2Se_3 films reduce both the T_C and the critical field (H_C) of the superconducting electrodes significantly.

II. EXPERIMENTAL RESULTS

Recent progress in thin film growth of TIs by molecular beam epitaxy (MBE) has made planar TI devices possible.[22–26] Our high-quality Bi_2Se_3 films were grown under Se-rich conditions on sapphire (5 QL) and high-resistivity silicon (200 QL) substrates in ultrahigh-vacuum MBE systems. A scanning tunneling microscope (STM) image of a 5-QL sample is shown in the left inset of Fig. 1(a). The atomically flat morphology demonstrates the high crystal quality of the film. The carrier density and the mobility of the 5-QL film at 2 K are $\sim 4\times10^{18}$ cm^{-3} (2×10^{12} cm^{-2}) and 3320 cm^2/Vs by Hall measurement, respectively. With decreasing thickness of the film, the surface-to-volume ratio increases and surface properties should become more prominent. However, it has been shown by ARPES that in films with thickness of less than 5 QL, the interaction between top and bottom surfaces may destroy the topologically protected surface state.[23]

The right inset of Fig. 1(a) is a schematic diagram of our transport measurement structure. Superconducting In dots $\sim$0.5 mm in diameter and $\sim$0.2 mm thick are directly pressed onto the top surface of the Bi_2Se_3 film. The distance between the two electrodes is $\sim$1 mm. Figure 1(a) shows resistance as a function of temperature (R–T) for the 5-QL Bi_2Se_3 film. In this paper, unless noted otherwise, the magnetic field is always applied perpendicular to the film and the excitation current for the measurement is 50 nA (corresponding essentially to a zero-bias resistance measurement). From 300 to 45 K, the R–T

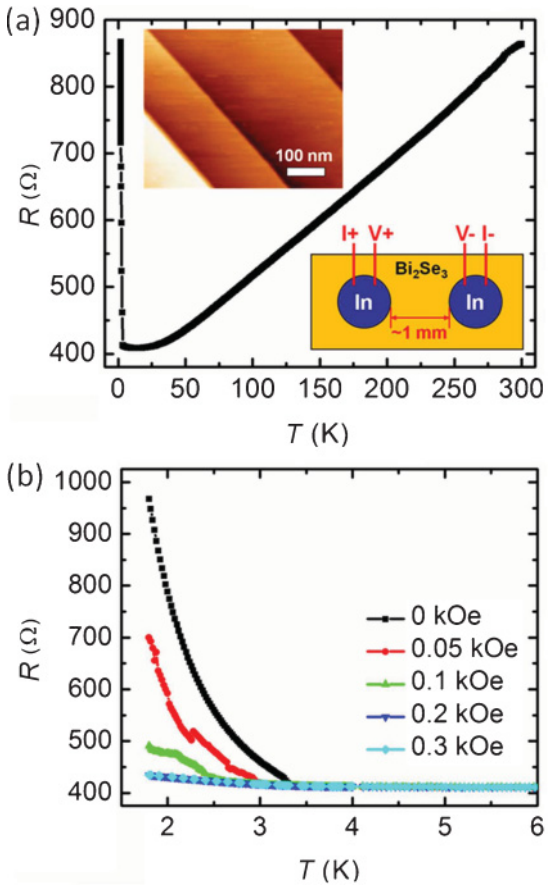

FIG. 1. (Color online) R–T behavior of the 5-nm-thick Bi_2Se_3 film contacted by two superconducting In dots. (a) R vs T of the 5-QL Bi_2Se_3 film from room temperature to low temperature. The left inset is a STM image of the Bi_2Se_3 film. The right inset is the measurement structure. (b) R vs T at different perpendicular fields. The curves at 0.2 and 0.3 kOe are superimposed.

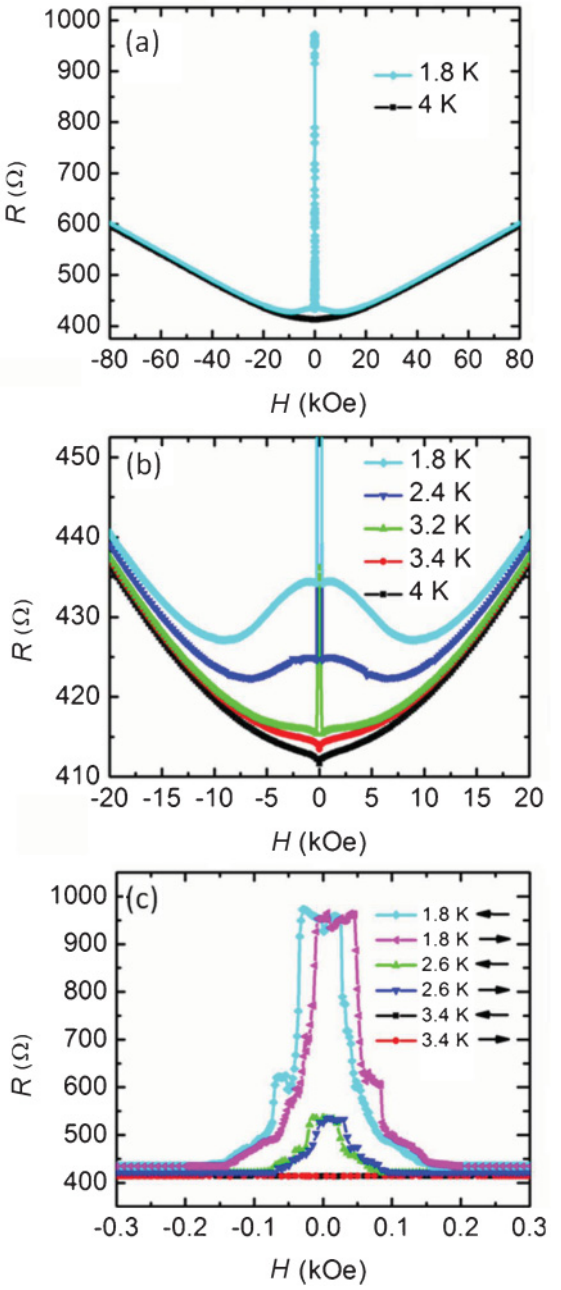

FIG. 2. (Color online) R–H scans of the 5-nm-thick Bi_2Se_3 film contacted by In electrodes. (a) Resistance as a function of perpendicular magnetic field at 4 and 1.8 K. (b) Magnified MR for several temperatures. (c) MR peaks near the zero field show terrace structure and hysteresis for scans made below T_C. The → arrow indicates the scan was made from a negative to a positive field.

curve shows linear metallic behavior. A resistance minimum is found near 13.3 K. The residual resistance ratio between 300 and 13.3 K is 2.1. Below 13.3 K, the resistance increases gradually with decreasing temperature. However, at 3.29 K (slightly below the T_C of bulk In, or 3.4 K), the resistance shows an abrupt increase. This resistance enhancement is shown in more detail in Fig. 1(b). The resistance at 1.8 K (967.23 Ω) is 2.34 times the resistance when the In electrodes are normal at $T = 3.4$ K. With an increasing field, this resistance enhancement decreases rapidly. When the field is 200 Oe, the enhancement behavior is suppressed. This means the actual critical field of the In electrodes here is lower than 200 Oe, which is the critical field of bulk In at 1.8 K. We interpret the enhancement in R to be a consequence of the onset of superconductivity of the In electrodes; however, it appears that the transition temperature and critical field of the In electrodes when contacting the Bi_2Se_3 film are slightly below the natural values.

Resistance as a function of the magnetic field (R–H) for the 5-QL Bi_2Se_3 film is shown in Fig. 2(a). At 4 K (above T_C of In), the R–H curve shows linear MR from 26 to 80 kOe. Such a linear MR has been attributed to the surface states with the linear energy–momentum correlation.[26,27] However, at 1.8 K (below T_C of In), near the zero field, the sample exhibits a striking MR peak. Between 0.2 and 9 kOe, well above the critical field of the electrodes, the resistance decreases unexpectedly with the field. Upon further increase in the magnetic field, the MR shows the same positive linear behavior as the R–H curve at 4 K.

Figure 2(b) shows MR in a small field at different temperatures in more detail. Above T_C of the In electrodes (at 3.4 and 4.0 K), we observe a positive MR. In addition, there is a small MR dip around the zero field, which has been studied

carefully and attributed to the weak antilocalization effects in TIs.[26,28] At temperatures below T_C of the In electrodes, the MR dip disappears and a sharp MR peak emerges. With decreasing temperature, the peak value increases rapidly, consistent with the R–T curves of Fig. 1. At 1.8 and 2.4 K, besides the sharp resistance peak around the zero field, an additional negative MR is observed from 200 Oe to 9 and 7 kOe, respectively. At lower temperatures, the negative MR is more robust. This result is unexpected. TI films contacted with normal metal electrodes show positive MR in a perpendicular field;[28] therefore, the negative MR cannot be from the TI film itself. However, if the observed negative MR is due to the superconductivity of In electrodes, we would not expect this behavior for fields larger than the H_C of the In electrodes (∼200 Oe at 1.8 K). Interestingly, this negative MR behavior extends up 9 kOe—but only at temperatures below T_C of the electrodes.

Figure 2(c) shows the details of the MR peak shown in Figs. 2(a) and 2(b). Under higher field resolution, the MR "peak" appears as a plateau with terraces. When we scan magnetic field from negative to positive values and then from positive back to negative values, the sample exhibits hysteretic behavior at 2.6 and 1.8 K. The plateau/terrace structure of the MR peak and the hysteresis are suggestive of a ferromagnetic response in the conduction electrons. There is no possibility of magnetic contamination in the process of sample preparation. A 3D image of the resistance as a function of field and temperature and the resistance contour map along the T–H axes, constructed from the experimental data we have obtained on this sample, are shown in Fig. 3. More details can be revealed in this figure. In addition to bulk In electrodes measurements, mesoscopic superconducting Al and W electrodes were patterned on the TI films to test the universality of the observed phenomena. The inset of Fig. 4(a) is a scanning electron microscope (SEM) image of our measurement structure. The Bi_2Se_3 film for this sample is 200 nm thick and grown on high-resistivity silicon substrate. The substrate is completely insulating below 150 K. The carrier density and the mobility of the film at 1.8 K are found to be 2.76×10^{18} cm^{-3} (5.52×10^{13} cm^{-2}) and 2800 cm^2/Vs by Hall measurement, respectively. The superconducting Al electrodes are 50 nm thick and directly deposited on the top surface of the film by electron beam lithography followed by electron-beam–assisted evaporation. The distance between the two Al electrodes is 1 μm. Figure 4(a) shows the R–T curves of this sample. Under a zero magnetic field, there is a sharp resistance increase at 0.95 K from 23.5 Ω, which becomes saturated below 0.85 K at 28.5 Ω. This enhancement is similar to our observation in the sample with bulk In electrodes. The onset temperature of the resistance enhancement at 0.95 K is significantly lower than the T_C of 50-nm-thick Al film. This enhancement is suppressed by a field of 100 Oe. An Al film of the same thickness that was evaporated with the same procedures on an insulating Si_3N_4 substrate shows a T_C of 1.4 K and a critical field of ∼800 Oe at 0.65 K. Thus, the superconductivity of the Al electrodes is substantially and clearly weakened by the TI film. As shown previously, the effect of the Bi_2Se_3 film on the bulk In electrodes is not as strong. This is not unreasonable, because the Al electrodes are only 50 nm thick and the In electrodes are "macroscopic" in size. The MR behavior in a small field, as shown in Fig. 4(b), is

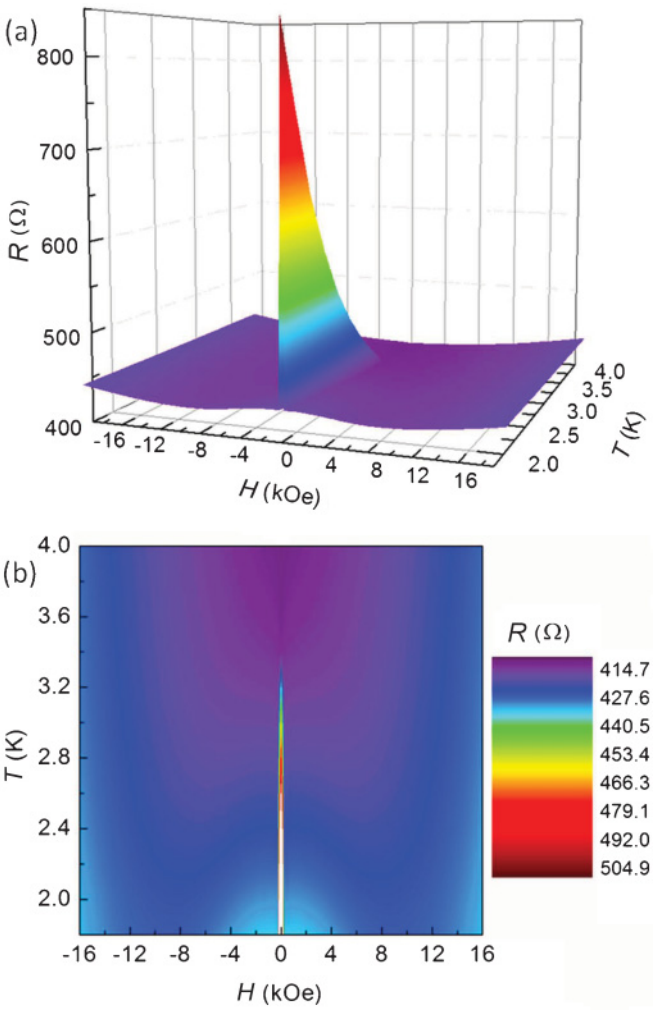

FIG. 3. (Color online) (a) 3D image of resistance as a function of the perpendicular field and temperature measured with a bias current of 500 nA for the 5-QL-thick Bi_2Se_3 film contacted by bulk In electrodes (In-Bi_2Se_3-In). A sharp resistance enhancement induced by the interaction between superconducting electrodes and Bi_2Se_3 film is found. (b) Color contour map of resistance along the temperature and perpendicular magnetic field axes of the 5-nm-thick Bi_2Se_3 film contacted by In electrodes. The colors represent resistance from 410 Ω (deep purple, the shade at the top of the color scale) to 510 Ω (deep red, the shade at the bottom of the color scale). White means the resistance is larger than 510 Ω.

similar to that found with In electrodes, as shown in Fig. 2(c). The observations in this Al electrode device were confirmed in two additional devices with the same geometry by a zero-bias differential resistance measurement, which was carried out using a lock-in amplifier with 100-nA alternating current excitation at a frequency of 97 Hz.

By means of the focused ion beam (FIB) deposition technique,[29–32] superconducting W electrodes were fabricated on the Bi_2Se_3 film [inset of Fig. 5(a)]. The thickness of the Bi_2Se_3 sample is also 200 nm, and the distance between two W electrodes is 1 μm. The FIB-deposited amorphous W strips have been used in a number of experiments as superconducting electrodes.[29–31] The T_C of the strips depends on the exact deposition parameters of the FIB process, but

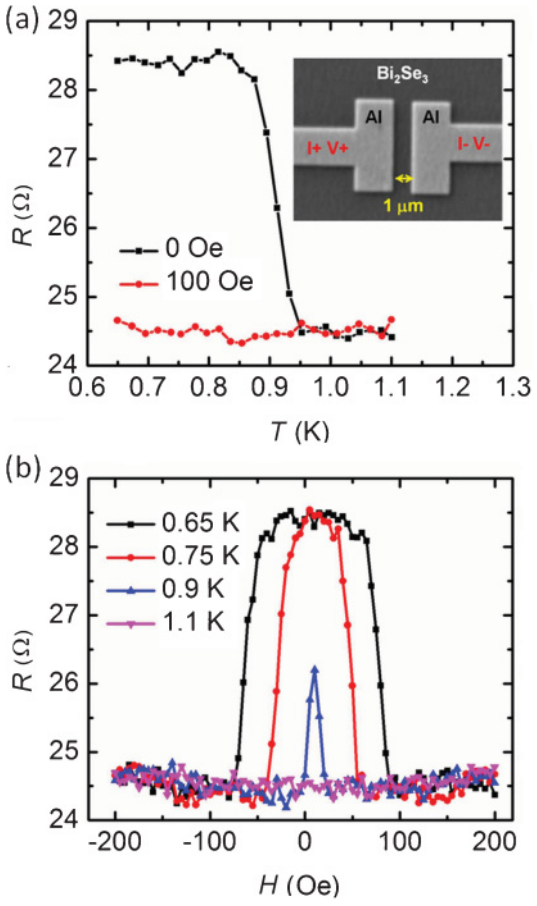

FIG. 4. (Color online) Transport behaviors of 200-nm-thick Bi_2Se_3 films contacted by superconducting Al electrodes. (a) A sharp resistance enhancement is seen at 0.95 K, which saturates below 0.85 K. An applied magnetic field of 100 Oe suppresses the enhancement. The inset is a SEM image of the Al contacts on the surface of the Bi_2Se_3 film. (b) The details of the MR in a small field. The resistance peak at 0.65 K is suppressed under a field of less than 100 Oe, which is much smaller than the H_C (800 Oe) of a 50-nm-thick Al film not contacting a Bi_2Se_3 film. The T_C of such an "isolated" Al film is 1.4 K.

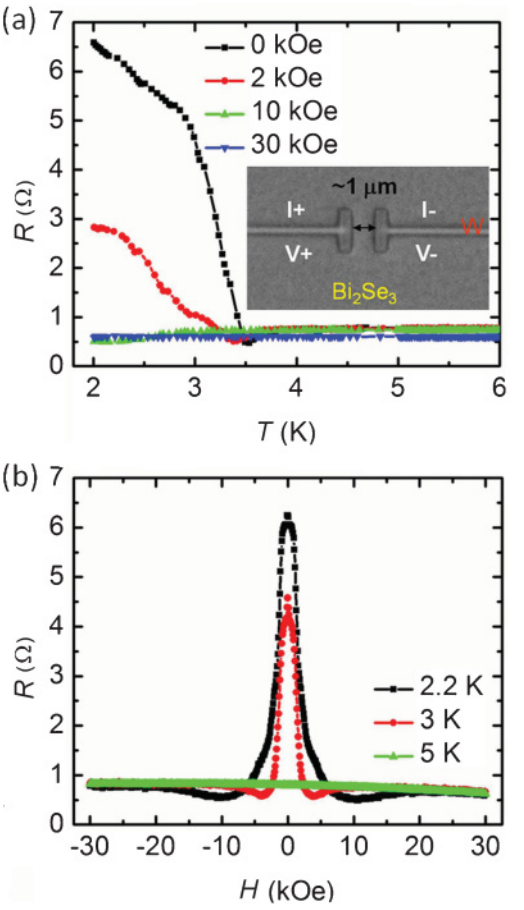

FIG. 5. (Color online) Transport behaviors of a 200-nm-thick Bi_2Se_3 film contacted by superconducting W electrodes. (a) R vs T scans under different magnetic fields. The inset is a SEM image of the W contacts on the surface of the Bi_2Se_3 film. (b) MR at different temperatures. When the W electrodes become superconducting, the MR shows a large peak around the zero field. This behavior disappears when the temperature is larger than the T_C. The resistance peak is suppressed under a field of ~10 kOe at 2.2 K, much smaller than the H_C of the W strips (80 kOe).

it was consistently found to be between 4 and 5 K when contacting metallic and magnetic nanowires.[29–32] This is much higher than the T_C of pure W (~12 mK), because the FIB-deposited W strips contain approximately 40% atomic carbon and 20% atomic gallium.[32] During the FIB deposition process, the top layers of the Bi_2Se_3 film are etched away, making fresh contact between the electrodes and the film. It has been shown that in the FIB process, electrically transparent interfaces were achieved.[30] Figure 5(a) shows the R–T curves of the W-Bi_2Se_3-W structure at different fields. The superconductivity-induced resistance enhancement is again seen in this structure. The resistance increases from 0.5 to 6.5 Ω when the W electrodes turned superconducting. The onset temperature of the resistance enhancement is ~3.5 K, which is again significantly smaller than the T_C (4–5 K) of the W strips.[29–31] The magnetic field sufficient to suppress the resistance peak is less than 10 kOe at 2.2 K, which is again much smaller than the H_C of the W strips (~80 kOe).[29,30] These results confirms the findings with In and Al electrodes that the Bi_2Se_3 film weakens the superconductivity of the contacting electrodes. The MR behavior shown in Fig. 5(b) is also consistent with that shown in Fig. 2. For MR scans made below T_C of W, in addition to the prominent peak at low field, a minimum in R is found at a field value above H_C of the specific temperature of the scan.

To further understand the interplay among the TI thin films with superconducting electrodes, we carried out differential conductance measurements. Figure 6(a) plots field-dependent I–V characteristics of the W-Bi_2Se_3-W sample at 0.5 K. There is a sudden voltage drop (negative conductance) when the field is less than 1.5 kOe in I–V curves. This phenomenon is not fully understood. Figure 6(b) shows bias-dependent differential conductance (dI/dV) of the same sample at different fields at 0.5 K. The negative dI/dV for small field ($H < 2$ kOe) is due to the voltage drop in Fig. 6(a). Apart from its negative value, the differential conductance in the zero field is also strongly suppressed below 0.33 mV (~$\Delta/2e$ of W, where Δ is the energy gap of the FIB-deposited W). This differential conductance suppression becomes weaker

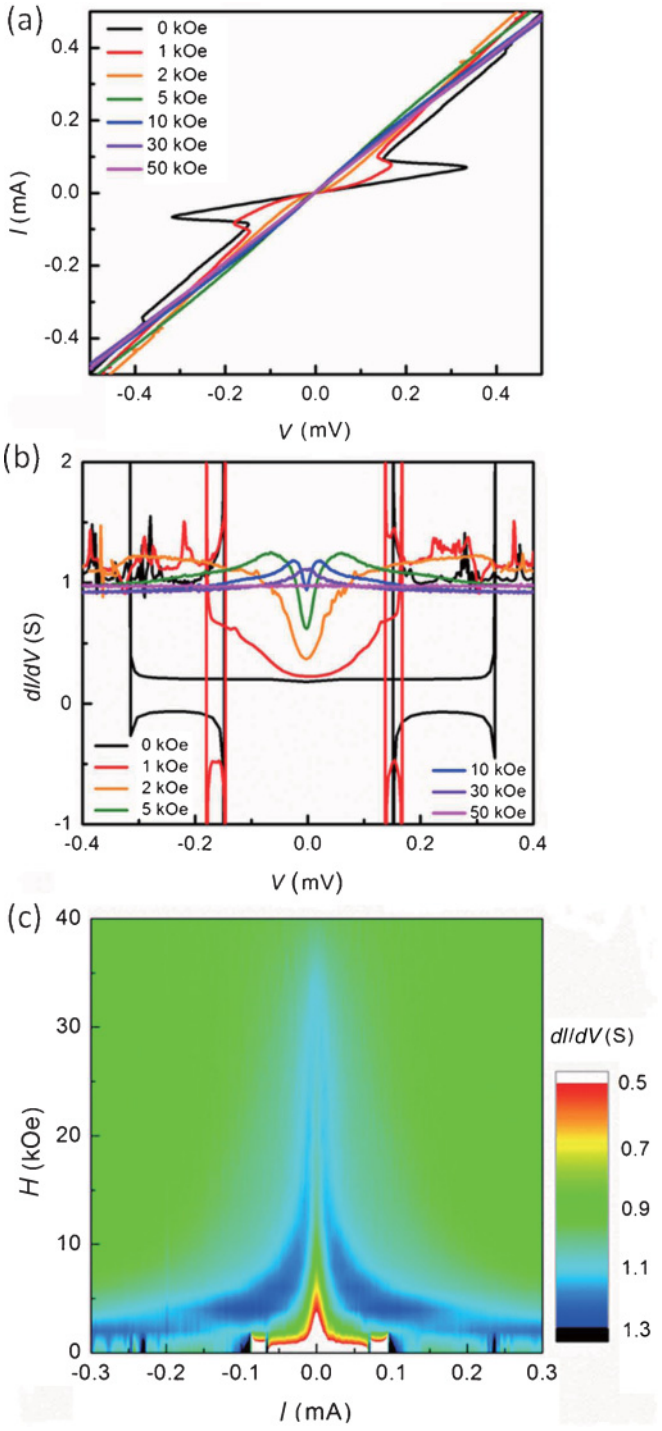

FIG. 6. (Color online) (a) I vs V at different perpendicular magnetic fields for the W-Bi_2Se_3-W sample at 0.5 K. (b) dI/dV vs V at different magnetic fields at 0.5 K. (c) dI/dV as a function of current I and field H at $T = 0.5$ K.

and moves to a lower bias as the field increases. At 30 kOe, the differential conductance switches from a suppression to an enhancement in a small bias regime. Finally, at 50 kOe, the dI/dV curve becomes a constant, which means the whole system becomes normal. In Fig. 6(c), we map out the variation of dI/dV as a function of current and magnetic field at 0.5 K. In a low-field and low-excitation current regime, the differential conductance is small, which is consistent with the observation of resistance upturn (Fig. 5). At a small current bias, with increasing field, the differential conductance first increases and then decreases. The dI/dV measurements confirm the observed resistance upturn behavior in such a W-Bi_2Se_3-W structure (Fig. 5).

III. DISCUSSION

The results shown here indicate that the phenomena we have observed are universal and reproducible: they are seen with three kinds of superconducting electrode materials, Bi_2Se_3 film thicknesses of 5 and 200 nm, and separation of the electrodes of 1 mm and 1 μm. The electrodes are attached onto the surface of the Bi_2Se_3 film by mechanical pressure (In), by electron-beam fabrication (Al) and by the FIB process (W).

If the contact between a superconductor and a normal metal is electrically transparent, the leakage of Cooper pairs into the normal metal can induce superconductivity in the normal metal. Simultaneously, the superconductivity of the superconductor on the other side of the interface can be weakened. This behavior is called the proximity effect.[33] While the observed weakening of the superconductivity of electrodes in our experiment is qualitatively consistent with this effect, the substantial decrease in T_C and H_C seen in the Al and W electrodes is unprecedented for superconducting electrodes contacting metallic,[29] ferromagnetic,[30] semiconducting nanowires,[34,35] and a two-dimensional graphene system.[36] The observed increase in R of the Bi_2Se_3 film when the electrodes turned superconducting is contrary to the conventional proximity effect interpretation and has not been observed in the half-metallic film employing the same measurement configuration.[37]

Extensive studies of transport across superconductor/semiconductor interfaces have shown a range of interesting behavior depending upon the transparency of the contact. When the interface is resistive, as typically occurs due to the formation of an interfacial Schottky barrier, an increased zero-bias resistance often accompanies the normal–superconducting transition of the electrode.[38] In past studies of various semiconductor–superconductor interfaces, such changes in resistance were readily understood using the Blonder-Tinkham-Klapwijk (BTK) model and extensions thereof,[39] wherein the interface transparency is a key factor in determining the temperature and bias dependence of the transport. Our observations, however, are quite different from those seen in all past measurements of semiconductor–superconductor junctions. First, they are robust against large variations in the transparency of the contacts. The resistances of the Bi_2Se_3 film we measured with the In, Al, and W electrodes are 425, 23.5, and 0.5 Ω in the normal state and 880, 28.5, and 6.5 Ω in the superconducting state, respectively. These values indicate that while the contacts with the In electrodes may be slightly resistive, the Al/Bi_2Se_3 and particularly the W/Bi_2Se_3 interfaces are electrically transparent. Despite the differences in the contact resistance of the three electrodes, the observed phenomena are essentially the same. Second, we find that the upturn in resistance can be strikingly large compared to that seen in past studies of semiconductor–superconductor junctions,[38,39] and it shows a behavior contrary to expectations from the BTK model.[40] We are particularly

surprised by our observation of the huge resistance upturn (1300%) for the W electrodes, as well as the strong suppression of differential conductance at low bias, thus unexpectedly showing the largest effect for the highest transparency contacts. Since we cannot explain our observations using the BTK model, which has been rigorously and extensively applied to a variety of semiconductor–superconductor junctions, we propose that the observed phenomenon is connected to the spin–helical surface states of the Bi_2Se_3 film; in addition, it may be a consequence of the entanglement of bulk and surface transport, because we cannot exclude the bulk transport channel in our measurements.

IV. CONCLUSION

A possible explanation of our observations reported here is that we are accessing the special property of TI surface states. The spins of the TI surface states are predicted to be helical with fixed spin orientation at a given momentum.[41] In our transport measurement configuration, the collective spin polarization of the TI surface state is aligned by the current.[42] When the electrodes become superconducting, the spin–singlet Cooper pairs are not compatible with the spin-polarized electrons on the TI surface. Spin flip processes must take place at the interface when the Cooper pairs leak from the current source electrode to TI and when the spin-polarized electrons flow from TI to the superconducting sink electrode. This process produces a sharp resistance enhancement below T_C. The spin-polarized current in turn strongly weakens the superconductivity of the superconducting electrodes. Recently, transport measurements with superconducting electrodes were also made on Bi_2Se_3 nanoribbons[43] and flakes,[16,44] showing a proximity effect and a downturn of zero-bias resistance. There are two possible explanations for the different behavior between the observations reported here and those reported with nanoribbons or flakes: First, the "minimally processed" samples used in our study could allow better preservation of the spin–momentum locked surface states. Another possibility is that the measurements of nanoribbons and micron-sized flakes are carried out in a measurement geometry that is clearly different from the one used in the present paper: the former involves sample edges, whereas the latter does not. Whatever the correct explanation for these observations, we believe that a systematic comparative study between these geometries may hold an important clue to the coupling of superconducting states with TI states, which not only exhibits the proximity effect at the TI and superconductor interface[45] but also offers a platform in searching for Majorana fermions.[46,47]

ACKNOWLEDGMENTS

This work was supported by the Pennsylvania State University Materials Research Science and Engineering Center under US National Science Foundation Grant No. DMR-0820404, the National Basic Research Program of China (Grant No. 2012CB921300), the General Research Fund (Grant No. HKU 7061/10P) and Collaborative Research Fund (Grant No. HKU 10/CRF/08) from the Research Grant Council of the Hong Kong Special Administrative Region, the (Chinese) National Science Foundation, the Ministry of Science and Technology of China, the National Natural Science Foundation of China (Grant No. 11174007). We are grateful to J. Jain, X. Qi, S. Zhang, L. Fu, C. Liu, Y. Ran, and M. Tian for illuminating discussions.

*jianwangphysics@pku.edu.cn
†chan@phys.psu.edu

[1] X. L. Qi and S. C. Zhang, Phys. Today **63**, 33 (2010).
[2] M. Z. Hasan and C. L. Kane, Rev. Mod. Phys. **82**, 3045 (2010).
[3] M. Z. Hasan and J. E. Moore, Annu. Rev. Condens. Matter Phys. **2**, 55 (2011).
[4] X. L. Qi and S. C. Zhang, Rev. Mod. Phys. **83**, 1057 (2011).
[5] L. Fu, C. L. Kane, and E. J. Mele, Phys. Rev. Lett. **98**, 106803 (2007).
[6] L. Fu and C. L. Kane, Phys. Rev. B **76**, 045302 (2007).
[7] J. E. Moore and L. Balents, Phys. Rev. B **75**, 121306(R) (2007).
[8] R. Roy, Phys. Rev. B **79**, 195321 (2009).
[9] D. Hsieh, D. Qian, L. Wray, Y. Xia, Y. S. Hor, R. J. Cava, and M. Z. Hasan, Nature **452**, 970 (2008).
[10] H. Zhang, C. X. Liu, X. L. Qi, X. Dai, Z. Fang, and S. C. Zhang, Nat. Phys. **5**, 438 (2009).
[11] Y. Xia, D. Qian, D. Hsieh, L. Wray, A. Pal, H. Lin, A. Bansil, D. Grauer, Y. S. Hor, R. J. Cava, and M. Z. Hasan, Nat. Phys. **5**, 398 (2009).
[12] J. G. Checkelsky, Y. S. Hor, M.-H. Liu, D.-X. Qu, R. J. Cava, and N. P. Ong, Phys. Rev. Lett. **103**, 246601 (2009).
[13] H. Peng, K. Lai, D. Kong, S. Meister, Y. Chen, X. L. Qi, S. C. Zhang, Z. X. Shen, and Y. Cui, Nat. Mater. **9**, 225 (2010).
[14] J. G. Analytis, R. D. McDonald, S. C. Riggs, J. H. Chu, G. S. Boebinger, and I. R. Fisher, Nat. Phys. **6**, 960 (2010).
[15] F. Xiu, L. He, Y. Wang, L. Cheng, L. T. Chang, M. Lang, G. Huang, X. Kou, Y. Zhou, X. Jiang, Z. Chen, J. Zou, A. Shailos, and K. L. Wang, Nat. Nanotech. **6**, 216 (2011).
[16] B. Sacepe, J. B. Oostinga, J. Li, A. Ubaldini, N. J. G. Couto, E. Giannini, and A. F. Morpurgo, Nat. Comm. **2**, 575 (2011).
[17] H. T. He, G. Wang, T. Zhang, I. K. Sou, G. K. L. Wong, J. N. Wang, H. Z. Lu, S. Q. Shen, and F. C. Zhang, Phys. Rev. Lett. **106**, 166805 (2011).
[18] H. Steinberg, D. R. Gardner, Y. S. Lee, and P. Jarillo-Herreo, Nano Lett. **10**, 5032 (2010).
[19] D. X. Qu, Y. S. Hor, J. Xiong, R. J. Cava, and N. P. Ong, Science **329**, 821 (2010).
[20] D. Hsieh, Y. Xia, D. Qian, L. Wray, J. H. Dil, F. Meier, J. Osterwalder, L. Patthey, J. G. Checkelsky, N. P. Ong, A. V. Fedorov, H. Lin, A. Bansil, D. Grauer, Y. S. Hor, R. J. Cava, and M. Z. Hasan, Nature **460**, 1101 (2009).
[21] Z.-H. Pan, E. Vescovo, A. V. Fedorov, D. Gardner, Y. S. Lee, S. Chu, G. D. Gu, and T. Valla, Phys. Rev. Lett. **106**, 257004 (2011).
[22] G. Zhang, H. Qin, J. Teng, J. Guo, Q. Guo, X. Dai, Z. Fang, and K. Wu, Appl. Phys. Lett. **95**, 053114 (2009).
[23] Y. Zhang, K. He, C. Z. Chang, C. L. Song, L. L. Wang, X. Chen, J. F. Jia, Z. Fang, X. Dai, W. Y. Shan, S. Q. Shen, Q. Niu, X. L. Qi, S. C. Zhang, X. C. Ma, and Q. K. Xue, Nat. Phys. **6**, 584 (2010).

[24]H. D. Li, Z. Y. Wang, X. Kan, X. Guo, H. T. He, Z. Wang, J. N. Wang, T. L. Wong, N. Wang, and M. H. Xie, New J. Phys. **12**, 103038 (2010).
[25]A. Richardella, D. M. Zhang, J. S. Lee, A. Koser, D. W. Rech, A. L. Yeats, B. B. Buckley, D. D. Awschalom, and N. Samarth, Appl. Phys. Lett. **97**, 262104 (2010).
[26]J. Wang, A. M. DaSilva, C. Z. Chang, K. He, J. K. Jain, N. Samarth, X. C. Ma, Q. K. Xue, and M. H. W. Chan, Phys. Rev. B **83**, 245438 (2011).
[27]H. Tang, D. Liang, R. L. J. Qiu, and X. P. A. Gao, ACS Nano **5**, 7510 (2011).
[28]J. Chen, H. J. Qin, F. Yang, J. Liu, T. Guan, F. M. Qu, G. H. Zhang, J. R. Shi, X. C. Xie, C. L. Yang, K. H. Wu, Y. Q. Li, and L. Lu, Phys. Rev. Lett. **105**, 176602 (2010).
[29]J. Wang, C. T. Shi, M. L. Tian, Q. Zhang, N. Kumar, J. K. Jain, T. E. Mallouk, and M. H. W. Chan, Phys. Rev. Lett. **102**, 247003 (2009).
[30]J. Wang, M. Singh, M. Tian, N. Kumar, B. Liu, C. Shi, J. K. Jain, N. Samarth, T. E. Mallouk, and M. H. W. Chan, Nat. Phys. **6**, 389 (2010).
[31]A. Sheilos, W. Nativel, A. Kasumov, C. Collet, M. Ferrier, S. Gueron, R. Deblock, and H. Bouchiat, Europhys. Lett. **79**, 57008 (2007).
[32]E. S. Sadki, S. Ooi, and K. Hirata, Appl. Phys. Lett. **85**, 6206 (2004).
[33]P. G. Gennes, Rev. Mod. Phys. **36**, 225 (1964).
[34]J. A. van Dam, Y. V. Nazarov, E. P. A. M. Bakkers, S. De Franceschi, and L. P. Kouwenhoven, Nature **442**, 667 (2006).
[35]J. Xiang, A. Vidan, M. Tinkham, R. M. Westervelt, and C. M. Lieber, Nat. Nano. **1**, 208 (2006).
[36]H. B. Heersche, P. Jarillo-Herrero, J. B. Oostinga, L. M. K. Vandersypen, and A. F. Morpurgo, Nature **446**, 56 (2007).
[37]R. S. Keizer, S. T. B. Goennenwein, T. M. Klapwijk, G. Miao, G. Xiao, and A. Gupta, Nature **439**, 825 (2006).
[38]A. Kastalsky, A. W. Kleinsasser, L. H. Greene, R. Bhat, F. P. Milliken, and J. P. Harbison, Phys. Rev. Lett. **67**, 3026 (1991).
[39]T. Schapers, *Superconductor–Semiconductor Junctions* (Springer Tracts in Modern Physics, Springer, Julich, 2001).
[40]G. E. Blonder, M. Tinkham, and T. M. Klapwijk, Phys. Rev. B **25**, 4515 (1982).
[41]X. L. Qi, T. L. Hughes, and S. C. Zhang, Phys. Rev. B **78**, 195424 (2008).
[42]S. Raghu, S. B. Chung, X. L. Qi, and S. C. Zhang, Phys. Rev. Lett. **104**, 116401 (2010).
[43]D. Zhang, J. Wang, A. M. DaSilva, J. S. Lee, H. R. Gutierrez, M. H. W. Chan, J. Jain, and N. Samarth, Phys. Rev. B **84**, 165120 (2011).
[44]F. Yang, Y. Ding, F. Qu, J. Shen, J. Chen, Z. Wei, Z. Ji, G. Liu, J. Fan, C. Yang, T. Xiang, and L. Lu, e-print arXiv:1105.0229 (2011).
[45]T. D. Stanescu, J. D. Sau, R. M. Lutchyn, and S. Das Sarma, Phys. Rev. B **81**, 241310(R) (2010).
[46]L. Fu and C. L. Kane, Phys. Rev. Lett. **100**, 096407 (2008).
[47]J. D. Sau, R. M. Lutchyn, S. Tewari, and S. Das Sarma, Phys. Rev. B **82**, 094522 (2010).